

## RESEARCH ARTICLE

# Structure Size Optimization and Magnetic Circuit Design of Permanent Magnet Levitation System Based on Halbach Array

FAZHU ZHOU<sup>1,2</sup>, JIE YANG<sup>1,2</sup>, AND LIMIN JIA<sup>1,3</sup><sup>1</sup>School of Electrical Engineering and Automation, Jiangxi University of Science and Technology, Ganzhou, Jiangxi 341000, China<sup>2</sup>National Innovation Center for Rare Earth Functional Materials, Ganzhou, Jiangxi 341000, China<sup>3</sup>State Key Laboratory of Rail Transit Control and Safety, Beijing Jiaotong University, Beijing 100044, China

Corresponding author: Jie Yang (245181082@qq.com)

This work was supported by the National Natural Science Foundation of China under Grant 52262050 and Grant 62063009.

**ABSTRACT** To utilize the load-bearing potential of permanent magnetic levitation (PML) structures and improve the levitation efficiency of rare-earth permanent magnetic materials, firstly, the number of magnetic blocks per unit wavelength and the correction factor of magnetic induction strength are introduced to establish an analytical model of vertical levitation force for the PML system based on Halbach arrays, which can effectively make up for the lack of precision caused by the production and installation of permanent magnetic arrays. Secondly, a method to optimize the dimensional parameters of the magnetic track structure combining quantitative analysis and multi-parameter optimization is proposed. Thirdly, a new permanent magnetic levitation structure with high levitation efficiency is designed. The experimental results show that the maximum error between the analytical model and the finite element calculation results is about 5.50% and the minimum error is 0%. The proposed magnetic circuit optimization structure improves the levitation efficiency by 4.60% and the ratio of levitation force to lateral deflection force by 2.48% compared with the “red track”. This study provides good reference for the design of permanent magnet magnetic levitation systems.

**INDEX TERMS** Permanent magnet magnetic levitation systems, structural size optimization, magnetic circuit design, Halbach array, parse mode.

## I. INTRODUCTION

Electromagnetic Suspension (EMS) and the Electrodynamic Suspension (EDS) are currently one of the two most developed suspension technologies in the field of Maglev trains [1], [2]. However, EMS has the disadvantage of high levitation energy consumption, while EDS cannot achieve static or low-speed levitation. Permanent magnetic levitation (PMS) is the third magnetic levitation technology system proposed after EMS and EDS. Comparing EMS and EDS, PMS has the advantages of low suspension energy consumption, static levitation, and low operation and maintenance costs [3], [4].

The associate editor coordinating the review of this manuscript and approving it for publication was Jesus Felez<sup>1b</sup>.

Despite the advantages that permanent magnetic levitation has; the development of permanent magnetic levitation technology was slow due to the limitation of the technology and magnet capacity of production at the early stage of development. In 1979, the introduction of the Halbach [5], [6] array has further advanced the development of the permanent magnetic levitation technology, making it widely used in the field of magnetic levitation transportation [7]. “China 01” proposed by China [8], “Sky Tran” [9] proposed by Israel and the new high-efficiency permanent magnetic levitation system-red rail [10] proposed by Jiangxi University of Science and Technology, are all typical applications of permanent magnetic levitation technology in the field of rail transport. Among them, the demonstration line, “red track”, the operated transportation project proposed by

Jiangxi University of Science and Technology was completed in Xingguo county, Jiangxi province in August 2022, which is expected to realize the commercial operation of permanent magnetic levitation rail transportation as shown in Fig. 1. Nowadays, rare-earth permanent magnetic materials have become important materials in rail transportation, aviation industry and national defense etc. It is important to improve the efficiency of rare-earth permanent magnetic levitation and reduce the cost of permanent magnetic levitation by designing the magnetic circuit and optimizing the structure size of Halbach permanent magnetic levitation system.



**FIGURE 1.** Xingguo permanent magnetic levitation project demonstration line “Red Rail” V2.0.

The analysis of Halbach array levitation force and the designing optimization of magnetic rail spacial structure are important technical aspects in engineering applications of permanent magnetic levitation rail transportation, and the correct expression of the magnetic force using mathematical model is the basic of levitation force analysis and magnetic rail optimization design. However, the levitation force of repulsive parallel Halbach arrays is often difficult to calculate accurately. Currently, there are two main approaches for modeling the magnetism of Halbach arrays, which are the surface current assumption method and the magnetic charge method [11], [12]. In [13] and [14], the authors attempted to model the magnetic force between permanent magnets by the use of the surface current hypothesis method, but its accurateness has not been verified by empirical data. In [15] and [16], the suction and repulsion models of Halbach arrays were developed to analyze the suspension gap effects and magnetic dimension parameters on magnetic force, respectively. In [17] and [18], a repulsive permanent magnetic levitation system has been designed by using Halbach arrays, and mathematical models for the levitation forces of three sets of Halbach arrays have been derived. In [19], a trapezoidal Halbach array model was computed by using an improved equivalent analysis method, which is easy to compute and highly accurate. In [20], for the difficult problem of predicting the levitation force of hybrid electromagnetic structures with Halbach arrays, original stochastic algorithm was corrected by using the normal

distribution parameter, which improved the accuracy of the prediction model.

All of the above research results have shortcomings. On one hand, the mathematical analytical models based on the derivation under equivalent or idealized conditions lack the verification of physical measurements. On the other hand, it is often difficult for the above models to accurately represent the actual levitation system due to the limitation of the production and installation accuracy of the magnetic track in the actual permanent magnet levitation system. To make up for the above deficiencies, the structural dimension optimization and magnetic circuit design problems of permanent magnet magnetic levitation systems with Halbach arrays are investigated in this manuscript through three contributions: 1. By introducing the number of magnetic blocks per unit wavelength and the correction coefficient of magnetic induction strength in the analytical model, the case of multiple arrays can be expressed, and the problem of insufficient accuracy due to the production and installation of permanent magnetic arrays can be effectively compensated. 2. A method of size optimization of the magnetic track structure with quantitative analysis and multi-objective optimization is proposed, which improves the efficiency of optimizing the size of the permanent magnetic levitation structure. 3. A non-standardized array structure is designed to effectively improve the levitation efficiency of the permanent magnetic levitation system.

This paper takes the parallel Halbach array permanent magnetic levitation system as the main research object, and establishes the analytical model based on the molecular current surface method, aimed at revealing the law of influence of the levitating air gap and the size of permanent magnet on the levitation force, and optimize the size parameters of Halbach array magnetic track structure by mathematical analysis method, based on which the performance of several levitation structures are compared and analyzed by simulation. The structure of this paper is as follows: In section II, the modeling process of parallel five-group Halbach array levitation force is described in detail considering the length, width and thickness of levitation air gap and levitation magnetic block, and the simulation verification of Halbach array levitation force and lateral force is carried out by using finite element analysis method to test the validity of the model. In section III, the law of influence of Halbach array block width and thickness on the levitation force is explored by mathematical model analysis combined with finite element method (FEM), and the relationship between block width and thickness and the efficiency of levitation is discussed, and the optimized dimensional parameters are given. In Section IV, several levitation structures are designed, simulated, compared and analyzed based on the results of optimizing the structural size of the levitation system in Section III, combined with the engineering requirements of “Red Rail” in Xingguo county, the first domestic maglev air rail engineering demonstration line developed by our teams. In Section V, conclusions are given.

**II. SUSPENSION FORCE MODEL AND ITS VALIDATION**

In order to improve the levitation efficiency of permanent magnetic levitation and accelerate the application process of permanent magnetic levitation technology, a method using five groups of Halbach array repulsive levitation structure is proposed in the development of Red Track V2.0 system, and the levitation structure schematic diagram is shown in Fig. 2. In this paper, the Halbach array levitation structure shown in Fig. 2 is used to establish its mathematical model by combining surface current assumption and numerical fitting based on the following assumptions.

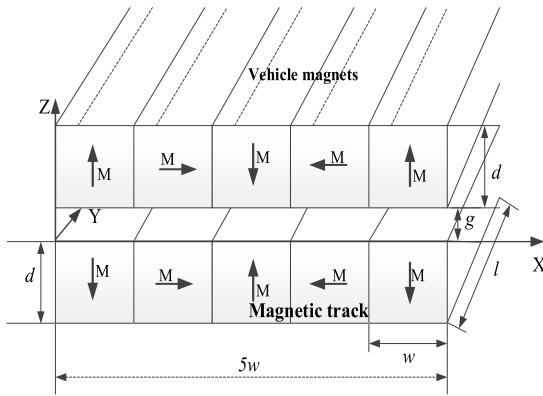


**FIGURE 2.** Schematic diagram of Halbach's permanent magnetic levitation system.

- a. The magnetic track is infinitely long in the y-axis direction, ignoring end effects.
- b. Permanent magnet material with high remanent magnetism.
- c. Ignore the effect of weak side.
- d. The on-board magnets are installed perfectly symmetrical to the magnetic rails, and the magnetic induction is equal along the y-axis direction, i.e.  $B(x_0, y, z_0)$  is constant.

During the magnetization of a permanent magnet material, the magnetization electro-fluid density can be expressed as follow:

$$\vec{J} = \nabla \times \vec{M} \tag{1}$$

where  $\vec{J}$  is magnetized electro-fluid density and  $\vec{M}$  is the dielectric magnetization strength.

$$\vec{M} = \frac{\mu_r - 1}{\mu_0 \mu_r} \vec{B} \tag{2}$$

where  $\mu_0$  is the vacuum permeability and  $\mu_r$  is the relative permeability of the permanent magnet.

During the magnetization of a permanent magnet, the magnetization intensity is usually constant, so the current density inside the magnetized body is zero. The magnetization intensity varies inside the permanent magnet at the bond with the external air, so there is a surface current of certain intensity at the bond, and the surface current density can be expressed as below:

$$\vec{K}_s = -\vec{e}_n \times \vec{M} \tag{3}$$

where  $\vec{K}_s$  is the surface current density of the magnetized body,  $\vec{e}_n$  is the normal vector pointing to the vacuum position, and the magnetic force of the air magnetic field on the permeability magnetic material in the magnetic field can be expressed as follow:

$$\begin{aligned} \vec{F} &= \iiint_V \vec{J} \times \vec{B} dv + \iint_s \vec{K}_s \times \vec{B} ds \\ &= \iiint_V (\nabla \times \vec{M}) \times \vec{B} dv + \iint_s (-\vec{e}_n \times \vec{M}) \times \vec{B} ds \end{aligned} \tag{4}$$

Substituting (2) and (3) into equation (4), we get the following equation using vector operation:

$$\vec{F} = \frac{\mu_r - 1}{2\mu_0 \mu_r} \iiint_V \nabla \times \vec{B}^2 dv \tag{5}$$

According to (5), the suspension force in the Z-axis direction can be found through the vector gradient integral equation, which is as follow:

$$\vec{F} = \frac{\mu_r - 1}{2\mu_0 \mu_r} \iint_s \vec{B}^2 ds \tag{6}$$

According to the results of the study in Reference [21], the magnetic induction intensity on the reinforced side of the Halbach array permanent magnet set can be expressed as follow:

$$\begin{cases} B_0 = B_r m_1 n \pi^{-1} (1 - e^{-kd}) \sin(\frac{\pi}{n}) \\ B_x = B_0 \sin(kx) e^{-km_2 z} \\ B_z = B_0 \cos(kx) e^{-km_2 z} \end{cases} \tag{7}$$

where  $B_0$  is the magnetic induction on the reinforced side,  $B_x$  and  $B_z$  are the components of the magnetic induction on the reinforced side of the Halbach array along the X and Z axes, respectively,  $B_r$  is the residual magnetization of the permanent magnet,  $k$  is the number of wavelengths in the magnetic group of the Halbach array,  $k = 2\pi/\lambda$ ,  $\lambda$  is the wavelength of the permanent magnet, and  $\lambda = nw$ ,  $n$  is the number of blocks per unit wavelength,  $w$  is the width of the unit block,  $d$  is the thickness of the permanent magnet,  $w$  is the thickness of the magnet,  $m_1$  and  $m_2$  are both correction factors for the magnetic induction.

In practical engineering, in order to maintain the integrity of the Halbach array wavelength, a unitary magnetic block is usually added at the end of the array so that the total width of the array is  $(n + 1)w$ . Combining equations (6) and (7), the levitation force along the z-axis of the strengthened side of the array can be expressed as follow:

$$\begin{aligned} F_z &= \frac{1}{2\mu_0} \iint_s B_z^2 ds \\ &= \frac{1}{2\mu_0} \int_0^{(n+1)w} \int_0^y \left[ \frac{B_r m_1 (1 - e^{-kd}) \sin(\frac{\pi}{n}) \cos(kx)}{\frac{\pi}{n} \times e^{km_2 z}} \right]^2 dy dx \end{aligned}$$

$$= \frac{B_r^2 n m_1^2 y (1 - e^{-kd})^2 \sin^2(\frac{\pi}{n}) e^{-2kz}}{4\pi^2 \mu_0} \times \{n \cos[kw(n + 1)] \sin[kw(n + 1)] + 2\pi(n + 1)\} \quad (8)$$

when  $n = 4$  (both 5 groups of Halbach), the (8) can be expressed as follow:

$$F_z = \frac{10m_1^2 B_r^2 w y (1 - e^{-kd})^2 e^{-2km_2 z}}{\pi^2 \mu_0} \quad (9)$$

where  $y$  is the length in the Y-axis direction, (9) is the expression of the mathematical model of the suspension force. This model introduces the correction coefficients  $m_1$  and  $m_2$ , which can make up for the shortage of modeling under idealized conditions and enhance the reliability of the model.

This paper mainly studies the vertical levitation force mathematical model of the permanent magnet magnetic levitation system without considering the lateral deviation. In order to prevent the lateral deviation between the magnetic rail and vehicle magnet, the guiding wheels are used in building the vertical levitation force physical experiment test platform, so the force in the x-direction,  $F_x$ , is zero.

In order to verify the validity of the proposed mathematical model of suspension force, a combination of finite element analysis and actual measurement verification method was used to verify. Firstly, the finite element simulation model was established by using Ansoft Maxwell software, and static suspension force simulation experiments were conducted; secondly, combining the actual needs of the ‘‘Red Track V2.0’’ engineering demonstration line, the actual test platform was designed according to the parameters shown in Table 1, and experiments were conducted.

TABLE 1. Related parameters.

Quantity	Symbol	Value
thickness of magnetic block	$d$	25mm
length of magnetic block	$l$	600mm
magnetic block width	$w$	30mm
residual magnetism	$B_r$	1.35T
vacuum magnetic permeability	$\mu_0$	$4\pi \times 10^{-7} \text{H/m}$
relative magnetic permeability	$\mu_r$	1
orthodontic force	$H_c$	980KA/m
number of magnetic blocks in a unit	$n$	4
proportional correction factor	$m_1$	1.7635
correction factor for magnetic induction index	$m_2$	0.5181

In Table 1,  $d$ ,  $l$ ,  $w$  and  $n$  are the sizes of the physical structure of the Halbach array, which can be set according

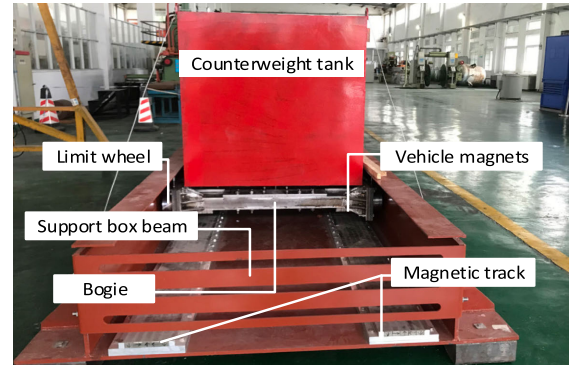


FIGURE 3. Suspension force test experiment site.

to the need.  $B_r$ ,  $\mu_r$  and  $H_c$  are the performance parameters of the permanent magnet material, and the values of different materials and grades of the permanent magnet material will be changed. In this paper, we choose the sintered NdFeB material, N45, and the values are as shown in Table 1.  $\mu_0$  is the vacuum permeability, and  $m_1$  and  $m_2$  are the proportionality and exponential correction coefficients, respectively, for the magnetic induction intensity.  $m_1$  and  $m_2$  are introduced to make up for the lack of precision due to the production and installation of permanent magnet arrays, and the specific values need to be combined with the actual levitation system test and determine. The permanent magnet material of grade NdFeB N45 was selected for the experiment, and the testing site is illustrated in Fig. 3. The experimental site consists of a bogie, a bilateral magnetic track, a counterweight tank and a support frame, in which the bogie consists of four vehicle magnets, each vehicle magnet is made of neodymium-iron-boron N45 material, the specific dimensions are shown in Table 1. The bogie is connected to the left and right sides of the four limit wheels to ensure that the bogie is only to do the pendant movement, and the counterweight slot in the bogie is on the top of the bogie in order to facilitate the adjustment of the load. The overall test scheme is as follows:

1.  $d$  are taken as 15mm, 25mm and 35mm respectively, and other parameters are shown in Table 1, The finite element simulation experiments are carried out with a suspension gap of 1mm as a step.

2. The sintered NdFeB material with the grade N45 is selected to build the physical levitation force test platform, as shown in Fig. 3. its model parameters are shown in Table 1.

3. The physical test experiment adopts the same step length as the finite element simulation (1mm step length), by adding load to the counterweight tank so that the suspension gap  $z$  changes in the range of 0-20mm. The weight of the counterweight tank is recorded once for every 1mm change to record the suspension force  $F_z$ .

The analytical model, finite element simulation and experimental results are shown in Fig. 4. Model represents the analytical model curve, FEM shows the simulation result of finite element model, and Experiment is the experimental

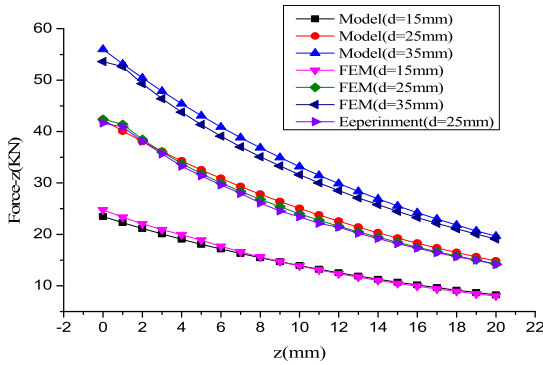


FIGURE 4. Analytical model and experimental curve.

result. From Fig. 4, it can be seen that the mathematical analytical model basically matches with the FEM calculation results and the experimental results. But there is a certain error between the analytical model and the FEM calculation results, and the smaller the  $z$  is, the larger the error is, and the maximum error is about 5.50%, which is caused by the simplification of the mathematical analytical model, ignoring the edge effect or the different meshes of the FEM simulation model. As can be seen from the Fig.4, the measured results are slightly smaller than the analytical model and finite element simulation results, with a maximum error of about 3.33%, caused by the production, processing and experimental assembly of the magnets.

### III. HALBACH ARRAY STRUCTURE SIZE OPTIMIZATION

The cost of magnetic material accounts for a large proportion of the cost of the whole permanent maglev rail transit system. It is important to improve the efficiency of permanent magnetic levitation and reduce the levitation cost under the condition of ensuring the levitation force and levitation gap. Magnetic circuit design and magnet structure size optimization are two technical routes to improve the efficiency of the permanent magnetic levitation, which are also important technical link for designing of permanent magnetic levitation rail transportation system [22]. However, the magnetic circuit design is largely influenced by design experience. Therefore, taking the route of permanent magnet structure size optimization is a good choice to improve the efficiency of permanent magnetic levitation.

It is easy to see from the levitation force expression (9) that the levitation force is proportional to the Length of vehicle magnet  $y$ , and the levitation force increases linearly with  $y$ . In the design process of suspension system, due to the limitation of actual route selection (such as small turning radius and large slope), the on-board permanent magnet can't be infinitely long, and its selection should be considered in combination with the turning radius and slope size, etc. Therefore, the length of the on-board permanent magnet is often not considered in the optimization of structural dimensions.

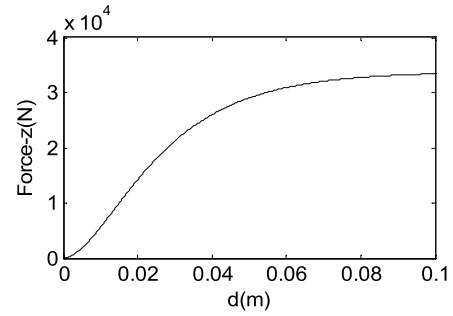


FIGURE 5. Curve of the effect of magnetic rail thickness  $d$  on suspension force.

#### A. OPTIMIZATION OF MAGNET THICKNESS $d$

From (9), it can be seen that the levitation force is not only related to the material of the permanent magnet itself, but also related to the thickness  $d$ , width  $w$ , Length of vehicle magnet  $y$  and levitation gap  $z$  of the permanent magnet. In order to study the effect of the thickness  $d$  of the permanent magnet on the levitation force, the quantitative analysis method is used with  $w = 30\text{mm}$ ,  $y = 600\text{mm}$ ,  $z = 15\text{mm}$ , and the other parameters except  $d$  are substituted into formula (9) according to the values shown in Table 1, and the following expressions are obtained.

$$F_z = \frac{0.504B_r^2 \times \left(1 - e^{-\frac{5\pi}{3}d}\right)^2 e^{-\frac{1}{4}\pi}}{\pi^2\mu_0} \quad (10)$$

Via equation (10), a two-dimensional curve can be plotted as shown in Fig. 5. It can be seen that the levitation force increases proportionally with the thickness  $d$ , but the slope of the curve gradually becomes smaller as  $d$  increases, and the increase in the slope of the levitation force gradually decreases.

The levitation force generated per unit of magnetic rail thickness can be expressed as

$$F_d = \frac{F_z}{d} = \frac{0.504B_r^2 \times \left(1 - e^{-\frac{5\pi}{3}d}\right)^2 e^{-\frac{1}{4}\pi}}{d\pi^2\mu_0} \quad (11)$$

The optimization objective of  $d$  is to maximize the value of  $F_d$ . In order to optimize  $d$  and increase the influence of the unit volume of permanent magnet on the levitation force, the derivative of (11) can be found as below:

$$\begin{aligned} \frac{\partial F_d}{\partial d} &= \frac{0.504B_r^2 e^{-\frac{1}{4}\pi}}{\pi^2\mu_0} \\ &\times \left( \frac{2 \times \frac{5\pi}{3}d \left(1 - e^{-\frac{5\pi}{3}d}\right) e^{-\frac{5\pi}{3}d} - \left(1 - e^{-\frac{5\pi}{3}d}\right)^2}{d^2} \right) \end{aligned} \quad (12)$$

According to equation (12), it can be plotted as shown in Fig. 6.  $F_d$  first increases and then decreases. When  $d$  varies in

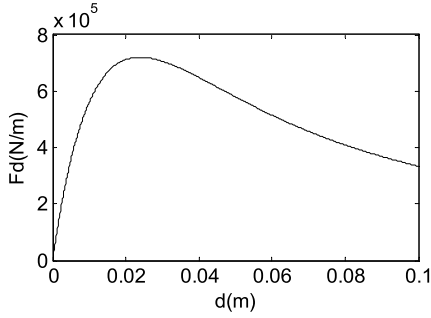


**FIGURE 6.** Curve of the effect of unit magnet thickness  $d$  on suspension force.

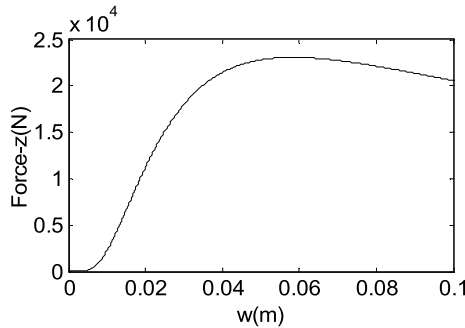


**FIGURE 7.** Curve of the effect of unit magnet width  $w$  on the suspension force.

the range of 0mm to 24mm, the suspension force generated per unit thickness first increases rapidly and then gradually decreases. In order to obtain the maximum value of  $F_d$ , let  $\partial F_d / \partial d = 0$  and solve the equation to get  $d = 0.0240$ , that is, under the condition of constant  $w$  and  $z$  ( $w = 30$  mm,  $z = 15$  mm),  $F_d$  gets the maximum value when  $d = 24$  mm, and the unit magnet thickness generates the maximum levitation force, which can complete the quantitative optimization target of thickness  $d$ .

### B. OPTIMIZATION OF MAGNET WIDTH $w$

Using the quantitative analysis method, take  $d = 25$  mm,  $y = 600$  mm,  $z = 15$  mm. Except  $w$ , other parameters as shown in Table 1. It can be substituted into the formula (9) and the following formula is obtained.

$$F_z = \frac{12m_1^2 B_r^2 w \left(1 - e^{-\frac{0.0125\pi}{w}}\right)^2 e^{-\frac{0.0125\pi}{2w}}}{\pi^2 \mu_0} \quad (13)$$

Referring to (13), a two-dimensional curve can be plotted as shown in Fig. 7.  $F_z$  increases as  $w$  increases, but the increase in the slope of the suspension force decreases as  $w$  increases.

In order to optimize the permanent magnet width and improve the influence of the unit permanent magnet width on the levitation force, the levitation force generated by the unit track width can be expressed as

$$F_w = \frac{F_z}{w} = \frac{12m_1^2 B_r^2 \left(1 - e^{-\frac{0.0125\pi}{w}}\right)^2 e^{-\frac{0.0125\pi}{2w}}}{\pi^2 \mu_0} \quad (14)$$

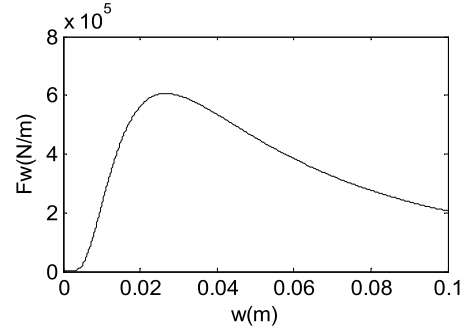


**FIGURE 8.** Curve of the effect of magnetic track width  $w$  on suspension force.

The optimization objective of  $w$  is to maximize the value of  $F_w$ . To maximize  $F_w$ , the derivative of (14) can be found as:

$$\begin{aligned} \dot{F}_w = \frac{\partial F_w}{\partial w} &= \frac{4.8 \times 10^3 m_1^2 \pi}{\pi^2 \mu_0 w^2} \times e^{-\frac{0.0125\pi}{2w}} \left(1 - e^{-\frac{0.0125\pi}{w}}\right) \\ &\times \left[3 \left(1 - e^{-\frac{0.0125\pi}{w}}\right) - 10\right] \end{aligned} \quad (15)$$

Let  $\dot{F}_w = 0$ , we can get  $w = 0.0268$ , which is when  $d = 25$ mm,  $z = 15$ mm,  $w = 26.8$ mm,  $w = 30$ mm, the maximum suspension force per unit thickness  $F_{w \max} = 649307$  N/m. According to equation (14), it can be plotted as shown in Fig. 8, with the increase of  $w$ , it shows a trend of increasing and then decreasing. When  $w$  varies in the range of 0 mm to 26.8 mm, it increases rapidly and then decreases gradually, that is with fixed thickness ( $d = 25$  mm) and suspension air gap ( $z = 15$  mm). The suspension force generated per unit magnet width is the largest when  $w$  is 26.8 mm, which completes the quantitative optimization of target  $w$ .

### C. COMPREHENSIVE OPTIMIZATION OF STRUCTURAL DIMENSIONS

From equation (9), it can be seen that the variation of the suspension force is affected by several parameters and there is an interaction between different parameters. Therefore, the optimization of the structure size of Halbach array cannot be analyzed from only one factor. The magnitude of the levitation force is proportional to the length  $y$  in the  $y$ -axis direction. But the length in the  $y$ -direction is often not considered in the design process of the engineering application of the actual magnetic circuit, and the core index is to use the least number of magnets to make the levitation force reach a predetermined value  $F_{z0}$  under a fixed levitation gap condition. Consequently, the core target parameters that need to be optimized for the structural dimensions of the Halbach permanent magnet track are  $w$  and  $d$ .

In order to observe the effect of  $w$  and  $d$  on the magnetic flux density, the magnetic flux density distribution is observed through the finite element simulation, and the experimental scheme is designed as follows:

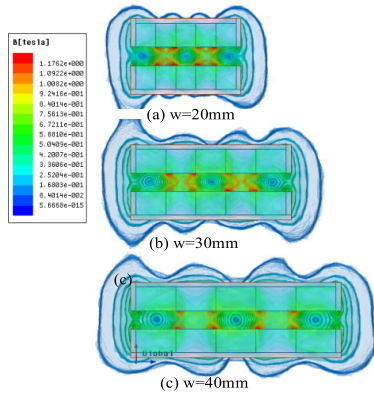


FIGURE 9. Flux density distribution at different track thicknesses.

a. With fixed  $w$  and  $z$  ( $w = 30 \text{ mm}$ ,  $z = 20 \text{ mm}$ ), 3 groups of different permanent magnet thicknesses ( $d = 15 \text{ mm}$ ,  $d = 25 \text{ mm}$ ,  $d = 35 \text{ mm}$ ) is selected for flux density simulation to observe the flux density variation, the simulation results are shown in Fig. 9;

b. With fixed  $d$  and  $z$  ( $d = 25 \text{ mm}$ ,  $z = 20 \text{ mm}$ ), flux density simulation was carried out, and three groups of different magnet widths  $w$  ( $w = 20 \text{ mm}$ ,  $w = 30 \text{ mm}$ ,  $w = 40 \text{ mm}$ ) were selected for flux density simulation experiments. The results are shown in Fig. 10.

As can be seen from Fig. 9, the flux density increases gradually with the Halbach magnet thickness  $d$ . The maximum flux density is mainly distributed in the suspension air gap of the two parallel Halbach arrays and concentrated in the middle of the symmetric array. Therefore, it can be concluded that with the magnet width and suspension air gap fixed, the flux density between the suspension air gaps increases proportionally with the permanent magnet thickness. Thus, the suspension force increases.

As can be seen from Fig. 10, when  $d$  and  $z$  are fixed, the maximum flux density is mainly distributed in the suspension air gap of the two parallel Halbach arrays and concentrated in the middle of the symmetric array. The maximum flux density distribution decreases slightly with the increase of the magnet width  $w$ . But the wider the magnet is, the more uniform the flux density in the suspension air gap becomes, the wider the magnetic peak is, and the flux increases. Therefore, it can be further shown that the magnetic flux and levitation force in the levitation air gap increase gradually with the permanent magnet width when the magnet width and levitation air gap are fixed.

To observe the effects of  $w$  and  $d$  on the suspension force more intuitively, the parameters other than  $w$  and  $d$  are substituted into equation (9) according to the values in the table, and a three-dimensional graph is drawn as shown in Fig. 11.

It can be seen from Fig. 11 that the levitation force tends to increase non-linearly with the increase of  $w$  and  $d$ . The levitation force generated by a unit volume of the permanent

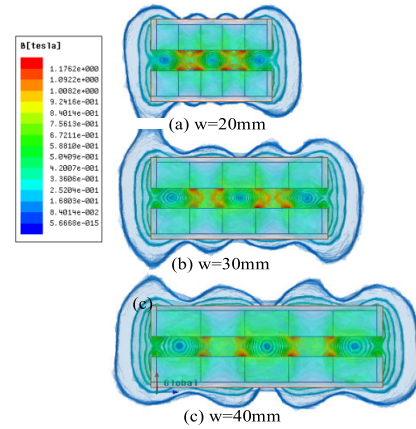


FIGURE 10. Flux density distribution at different track widths.

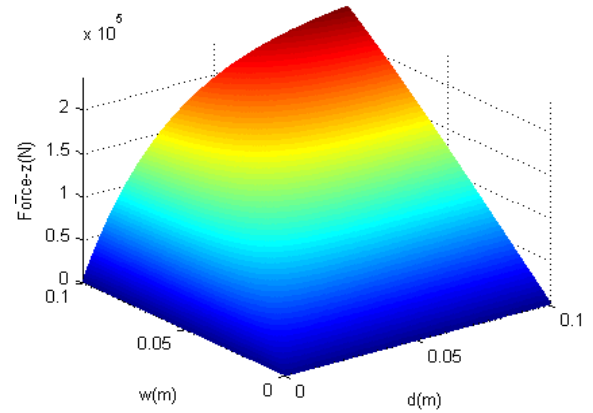


FIGURE 11. Three-dimensional graph of the levitation force and the width of the permanent magnet body thickness.

magnet can be expressed as:

$$F_{wd} = \frac{F_z}{ywd} = \frac{10m_1^2 B_r^2 w y_0 (1 - e^{-kd})^2 e^{-2km_2 z}}{\pi^2 \mu_0 w y d} \quad (16)$$

To achieve the optimization objectives of  $w$  and  $d$ , substituting the suspension objective ( $F_z = F_{z0}$ ,  $z = z_0$ ,  $y = y_0$ ) into equation (16), and it is obtained that:

$$F_{z0} = \frac{10m_1^2 B_r^2 w y_0 (1 - e^{-kd})^2 e^{-2km_2 z_0}}{\pi^2 \mu_0} \quad (17)$$

It can be obtained from equation (17) that:

$$d = -\frac{2w \ln \left( 1 - \sqrt{\frac{F_{z0} \pi^2 \mu_0}{10m_1^2 B_r^2 w y_0 e^{-\frac{\pi}{w} m_2 z_0}}} \right)}{\pi} \quad (18)$$

When  $F_z = F_{z0}$ , substituting (17) and (18) into (16) yields:

$$F_{wd} = \frac{F_z}{ywd} = \frac{-F_{z0} k}{y_0 w \ln \left[ \left( 1 - \sqrt{\frac{F_{z0} \pi^2 \mu_0}{10m_1^2 B_r^2 w y_0 e^{-\frac{\pi}{w} m_2 z_0}}} \right) \right]} \quad (19)$$

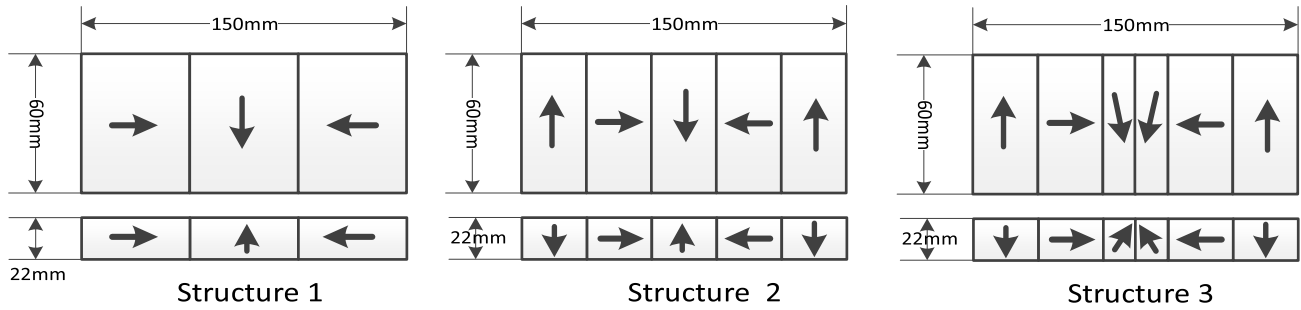


FIGURE 12. Schematic diagram of three different suspension structures.

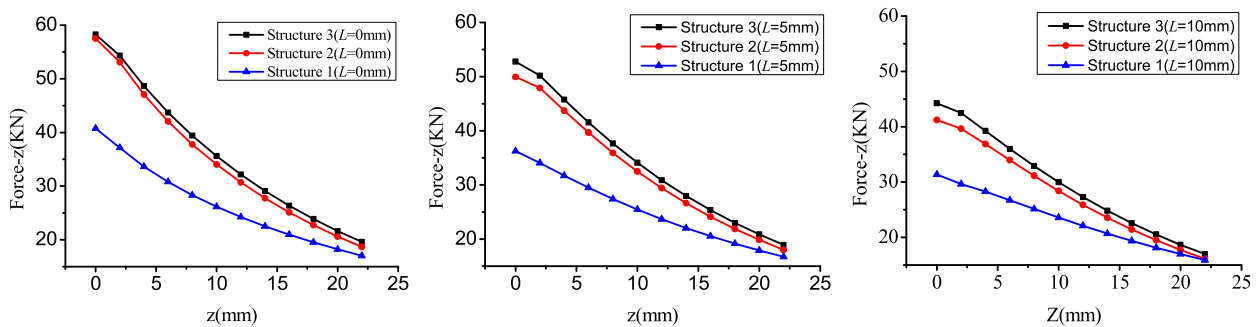


FIGURE 13. Comparison of suspension forces of several suspension structures under different lateral deflection displacements.

The derivative of equation (19) for  $w$ , let  $\partial F_{wd}/\partial w = 0$ , using Matlab to find  $w = 0.0381$ , substituting into equation (18) to get  $d = 0.0199$ , that is,  $w = 38.1\text{mm}$ ,  $d = 19.9\text{mm}$  take the maximum value, both with  $z = 15\text{mm}$  and  $F_{z0} = 17000\text{N}$  as the magnetic circuit design target, the size optimizing of  $w$  and  $d$  are  $38.1\text{mm}$  and  $19.9\text{mm}$  respectively, which completes the size optimization target. (18) and (19) are the Halbach array permanent magnet monomer size optimization formulas.

#### IV. SIMULATION CALCULATION AND COMPARATIVE ANALYSIS OF THREE SUSPENSION STRUCTURES

The levitation efficiency is the levitation force generated per unit of magnetic track volume. The levitation efficiency and levitation force/lateral force are two core indicators for the design of permanent magnetic levitation systems. Magnetic circuit design and optimization of magnetic track size parameters are two different technical routes to improve the levitation efficiency of rare-earth permanent magnet materials. The magnetic circuit design is to optimize the magnetic circuit by changing the shape, spatial combination and the magnetization direction of the permanent magnet monomer. Thus, improving the levitation efficiency of rare-earth permanent magnet materials, can efficiently reduce the magnetic losses and decrease the lateral deflection force.

According to the needs of the practical engineering, this paper designs the levitation structure 3 from the perspective

of magnetic circuit design with the following constraints as shown in Fig.12 (structure 3).

- The vertical levitation force is greater than or equal to the load target, both  $F_z \geq F_{z0}$  ( $F_{z0} = 17000\text{N}$ ).
- Maximum levitation efficiency  $F_{wd}$ .
- Minimum possible levitation force/lateral force.

In order to highlight the superiority of the proposed structure 3, the results of structure 3 are analyzed in comparison with those of structure 1 and 2. As shown in Fig. 12, among which Structure 1 is the levitation structure of the first permanent magnetic levitation testing line of Jiangxi University of Science and Technology, which adopts the 3-group Halbach array method, and the direction of magnetization of its magnetic blocks and the parameters of the structural dimensions are shown in the left-hand panel of Fig. 12. Structure 2 is the levitation structure of Xingguo permanent magnetic levitation rail transportation project demonstration line, which adopts the Halbach array with 5 groups, and the magnetization direction of the magnetic blocks is shown in the middle diagram of Fig. 12. Structure 3 is an optimized levitation structure with a symmetric 7-group Halbach array pattern, wherein the width of the two middle blocks is smaller and the magnetization direction is  $60^\circ$ , as shown in Fig.12 (structure 3). The volume of rare-earth permanent magnets used per unit length of magnetic track is equal in all three structures. The on-board magnets and the track magnets are sintered NdFeB of N52 and N45



TABLE 2. Comparison of suspension efficiency.

Suspension structure	Suspension efficiency N/m <sup>3</sup> (10mm)	Improvement rate	Suspension efficiency N/m <sup>3</sup> (15mm)	Improvement rate	Suspension efficiency N/m <sup>3</sup> (20mm)	Improvement rate
Structure 1	1.3214×10 <sup>7</sup>	-23.10%	1.0935×10 <sup>7</sup>	-18.16%	9.2079×10 <sup>6</sup>	-11.45%
Structure 2 (reference)	1.7183×10 <sup>7</sup>	0	1.3362×10 <sup>7</sup>	0	1.0399×10 <sup>7</sup>	0
Structure3	1.7974×10 <sup>7</sup>	4.60%	1.4066×10 <sup>7</sup>	5.27%	1.0923×10 <sup>7</sup>	5.04%

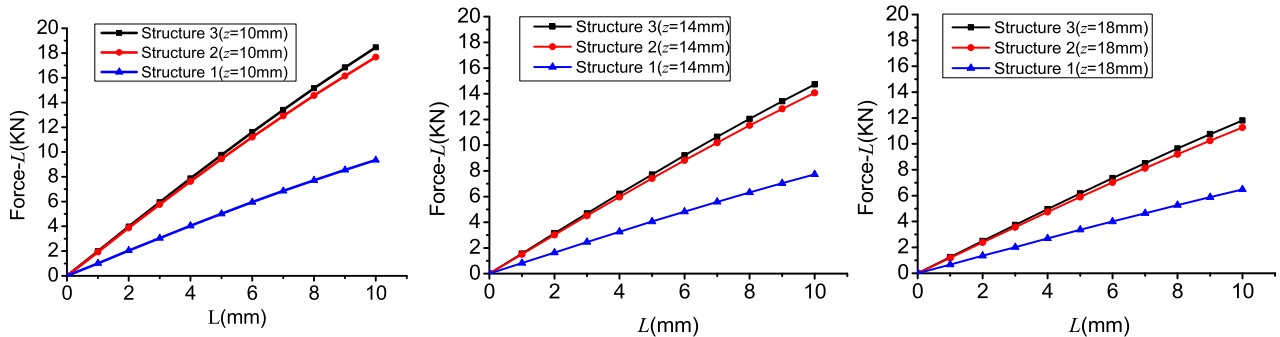


FIGURE 14. Comparison of lateral forces of several suspension structures with different suspension heights.

TABLE 3. Suspension/lateral deflection force.

Suspension structure	Suspension force / lateral deflection force (5 mm)	Improvement rate	Suspension force / lateral deflection force (10 mm)	Improvement rate
Structure 1	5.09	47.97%	2.52	56.52%
Structure 2 (reference)	3.44	0	1.61	0
Structure3	3.49	1.45%	1.65	2.48%

respectively. The length of on-board magnets is 600mm in all three structures, and the cross-sectional area of magnetic track is equal. In order to illustrate the suspension efficiency and lateral deflection force of three different structures, the suspension heights  $z = 10\text{mm}, 15\text{mm}, 20\text{mm}$  and the lateral deflection displacements  $L = 0\text{mm}, 5\text{mm}, 10\text{mm}$  were selected for the simulation analysis of suspension force and lateral force, and the simulation results are shown in Figure 13-14.

The simulation results shown in Fig. 13 illustrate that the levitation efficiency is influenced by the design of levitation structure. To illustrate the influence of levitation structure on levitation efficiency, the levitation heights of 10mm, 15mm and 20mm were selected for levitation efficiency comparison without side deflection, and the results are shown in Table 2. Among the above three levitation structures, the highest levitation efficiency is structure 3, followed by structure 2 and the lowest is structure 1 under the same unit volume of magnetic rails. Compared with structure 2, the levitation efficiency of structure 3 is increased by 4.60%, 5.27% and

5.04% when the levitation height is 10mm, 15mm and 20mm respectively.

The simulation results shown in Fig. 14 show that under different lateral deflection displacement and the different suspension height, the lateral deflection force of structure 3 and structure 2 are closer, and the lateral deflection force of structure 1 is the smallest. To compare the suspension force/side deflection force of the above three structures, the suspension height of 10mm and the lateral deflection displacement of 5mm and 10mm are selected for the comparison of suspension force/side deflection force, and the results are shown in Table 3. The magnitudes of suspension force/side deflection force are structure 1, structure 3 and structure 2 in order.

In summary, among the three suspension structures designed above, structure 3 has the largest suspension efficiency, which is 4.60% higher compared to structure 2 ( $z = 10\text{mm}$ ). Structure 1 has the largest suspension force/lateral deflection force, and structure 3 is the second largest. Structure 3 is better when considered comprehensively, but in the

actual engineering magnetic circuit design, the actual line track structure or box girder cost needs to be combined to complete the final design solution.

## V. CONCLUSION

In this study, the mathematical model of two parallel Halbach arrays is established by the surface current method, revealing the law of influence of the spatial structure size of Halbach parallel arrays on the levitation force. A method is proposed to optimize the structure size of Halbach array permanent magnets by using a combination of model analysis and finite element simulation calculation, providing a theoretical guidance for the magnetic circuit design and avoiding Halbach permanent magnet magnetic circuit design process of experience, blind trial and error, thus improving the efficiency of permanent magnet utilization. The results of the study showed that:

(1) The mathematical model of vertical levitation force of permanent magnet magnetic levitation (PMML) based on Halbach established in this paper on the basis of the surface current assumption method, and effectively introducing the method of correcting the correction coefficient of the electromagnetic induction force, the lack of installation accuracy of the PMML system is compensated, and provides the basic support for the structural optimization of the PMML system, which is of great significance for the popularization of the permanent magnetic levitation technology.

(2) The combination of quantitative analysis and multi-parameter optimization method proposed in this paper can quickly achieve the structure size optimization of Halbach PML system, and the structure 3 designed by the idea of magnetic circuit design has high levitation efficiency and levitation force/lateral force, which can provide reference for engineering application research of permanent magnet magnetic levitation (PMML) rail transit system and academic research in the field of magnetic levitation.

(3) In this paper, in order to improve the levitation efficiency and the magnitude of the levitation force/lateral deflection force of the permanent magnet magnetic levitation system (PMMLS), by establishing a vertical mechanics model of PMMLS based on Halbach array, on the basis of which, we propose a combination of quantitative and multi-parameter optimization, which can effectively improve the efficiency of the design and optimization of the PMMLS. The disadvantage is that the mathematical model does not take into account the misalignment of the magnetic track with the on-board magnets. The transverse displacements, rotations, and nodding points of the on-board magnets will be considered in the mathematical model in the future work, so as to widen the scope of application of the model.

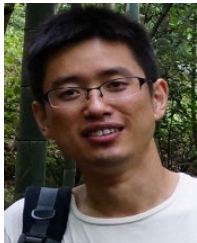
## REFERENCES

- [1] S. H. Liu, L. Wang, L. Z. Wang, and Q. L. Wang, "A review of research on electric levitating trains and on-board superconducting magnets," *J. Southwest Jiaotong Univ.*, vol. 4, no. 30, pp. 1–20, 2023.
- [2] Y. Wang, J. Yang, and Y. Cui, "Characterization of permanent magnetoelectromagnetic hybrid levitation guidance system for magnetic levitation trains," *Locomotive Electric Drive*, vol. 6, no. 1, pp. 1–8, 2021.
- [3] Z. Y. Guo and J. Yang, "DMC-PID control strategy for lateral force control system of permanent magnet suspension track," *J. Railway Sci. Eng.*, vol. 18, no. 6, pp. 1373–1381, 2021.
- [4] H. E. Liu, J. Q. Zou, and J. Yang, "Robust speed control of permanent magnetic levitating trains with self-tuning of adrc parameters," *J. Railway Sci. Eng.*, vol. 20, no. 9.
- [5] T. Gao, J. Yang, L. Jia, Y. Deng, W. Zhang, and Z. Zhang, "Design of new energy-efficient permanent magnetic Maglev vehicle suspension system," *IEEE Access*, vol. 7, pp. 135917–135932, 2019.
- [6] K. Halbach, "Design of permanent multipole magnets with oriented rare Earth cobalt material," *Nucl. Instrum. Methods*, vol. 169, no. 1, pp. 1–10, Feb. 1980.
- [7] N. X. Wang, D. X. Wang, K. S. Chen, and H. C. Wu, "Analytical model and design method of permanent magnet bearing load capacity based on Halbach array," *J. Mech. Eng.*, vol. 52, no. 3, pp. 128–135, 2016.
- [8] L. Q. Li, "Suspension rail permanent magnetic double suction balanced compensated suspension road car system," CN Patent 16 801 35A, 2005.
- [9] Y. Wiseman, "Safety mechanism for SkyTran tracks," *Int. J. Control Autom.*, vol. 10, no. 7, pp. 51–60, Jul. 2017.
- [10] J. Yang, T. Gao, Y. F. Deng, and B. Yang, "Research and design of permanent magnet magnetic levitation air rail system," *J. Railways*, vol. 42, no. 10, pp. 30–37, 2020.
- [11] Y. Chen and K. L. Zhang, "Analytic calculation of the magnetic field created by Halbach permanent magnets array," *Magn. Mater. Devices*, vol. 45, no. 1, pp. 1–9, 2014.
- [12] Y. Chen, "Characteristic analysis of electromagnetic forces created by low-speed PM electrodynamic suspension," Ph.D. dissertation, School Elect. Eng., Southwest Jiaotong Univ., Chengdu, China, 2015.
- [13] J. G. Ding, "Analysis of permanent magnet bearings based on equivalent current method," *Electromechanical Eng. Technol.*, vol. 50, no. 6, pp. 119–121, 2021.
- [14] W. Tang, L. Xiao, D. Xia, W. Yang, and Z. Wang, "2-D and 3-D analytical calculation of the magnetic field and levitation force between two Halbach permanent magnet arrays," *IEEE Trans. Magn.*, vol. 57, no. 4, pp. 1–8, Apr. 2021.
- [15] C. Luo, K. L. Zhang, and Y. Wang, "Stability control of permanent magnet electromagnetic hybrid Halbach array electric levitation," *J. Southwest Jiaotong Univ.*, vol. 57, no. 3, pp. 574–581, 2022.
- [16] H. F. Fang, J. Chen, J. H. Fan, and K. W. Xu, "Optimal design of Halbach square array adsorption mechanism," *Mech. Des. Manuf.*, vol. 5, no. 52, pp. 226–234, 2021.
- [17] Y. Jiang, Y. Deng, P. Zhu, M. Yang, and F. Zhou, "Optimization on size of Halbach array permanent magnets for magnetic levitation system for permanent magnet Maglev train," *IEEE Access*, vol. 9, pp. 44989–45000, 2021.
- [18] T. Gao, J. Yang, L. M. Jia, Z. L. Zhang, and Y. Y. Liu, "Study on dynamic characteristics of permanent magnet levitation system considering mechanical damping structure," *J. Railways*, vol. 43, no. 11, pp. 61–68, 2021.
- [19] B. Li, J. A. Zhang, X. L. Zhao, B. Liu, and H. Dong, "Research on air gap magnetic field characteristics of trapezoidal Halbach permanent magnet linear synchronous motor based on improved equivalent surface current method," *Energies*, vol. 16, pp. 793–804, Dec. 2023.
- [20] K. Hu, H. Jiang, S. Wang, and F. Li, "Magnetic force prediction of hybrid magnet with Halbach array using generalized regression neural network optimized by a modified Aquila optimizer," *Int. J. Appl. Electromagn. Mech.*, vol. 71, pp. 1–24, Jan. 2023.
- [21] S. H. Peng, H. D. Li, Z. Su, and Y. Y. Qu, "Sliding mode variable structure control of electric servo with uncertain parameters," *J. Electr. Mach. Control*, vol. 13, no. 1, pp. 128–132, 2009.
- [22] X. Jiang, "Modeling and magnetic field analysis of a new permanent magnet motor based on Halbach array pole structure," M.S. thesis, Hefei Univ. Technol., Hefei, China, 2021.



**FAZHU ZHOU** was born in Hainan, China, in 1986. He received the B.S. degree in transportation engineering and the M.S. degree in control engineering and control science from the Jiangxi University of Science and Technology, China, in 2009 and 2021, respectively, where he is currently pursuing the Ph.D. degree in maglev control.

From 2009 to 2015, he was a Research Assistant with the Applied Electronics Laboratory, Jiangxi University of Science and Technology. He teaches at the Jiangxi University of Science and Technology. Since 2016, he has been a Lecturer with the Department of Automation and the Deputy Director of the Electronics Application Laboratory. He is the author of one book *Innovative Research on the Application of Electronic Control Theory*, in 2021, more than ten articles, and more than ten inventions. His current research interests include magnetic levitation control, permanent magnet magnetic circuit design, and tunnel inspection technology.



**JIE YANG** was born in Anhui, China. He received the Ph.D. degree in rail transportation safety from Beijing Jiaotong University, in 2011. He is currently pursuing the Ph.D. degree with the School of Electricity, Jiangxi University of Science and Technology.

He is a high-level leading talent in Jiangxi, China, the Director of the Jiangxi University of Science and Technology Permanent Magnetic Levitation Technology and the Railway Transportation Research Institute, the Director of the Jiangxi Provincial Key Laboratory of Magnetic Levitation Technology, and the Secretary General of the China Rare Earth Society of Rare Earth Permanent Magnetic Levitation Technology and Application Specialized Committee, as a Technical Responsible Person to participate in the research and development of China's

independent intellectual property rights of the small-capacity magnetic levitation rail transit system, "Red Rail Magnetic Levitation." As a Technical Leader, he participated in the research and development of China's independent intellectual property rights of small capacity magnetic levitation rail transportation system "Red Rail Magnetic Levitation." He has published more than 50 articles and more than 30 inventions. His current research interests include magnetic levitation control, traction optimization, and artificial intelligence.



**LIMIN JIA** was born in Xinjiang, China, in 1963. He received the Ph.D. degree in automation and control in transportation from the China Academy of Railway Sciences, Beijing, China, in 1991.

He is currently a Professor and a Doctoral Supervisor with Beijing Jiaotong University, the Director of the Research Center for Intelligent Systems and Safety Technology, BJTU, the Chief Professor of the State Key Laboratory of Railway Control and Safety, and the Director of the Academic Committee of the Key Laboratory of Operational Active Safety Assurance and Risk Prevention and Control of the Railway Industry. He is also the executive director. He has published more than 200 articles and three books. He has made great contributions to the theory of intelligent control and intelligent automation in China and to the technology of railroad informatization. His current research interests include intelligent transportation systems, computational intelligence, and rail transportation control and safety.

...